



Best Time Domain Features for Early Detection of Faults in Rotary Machines Using RAT and ANN

Mohammed Al-Saad¹ · Mohammed Al-Mosallam¹ · Ahmad A. M. Alsahlani¹

Received: 14 November 2021 / Revised: 24 June 2022 / Accepted: 7 July 2022 / Published online: 2 September 2022
© Krishtel eMaging Solutions Private Limited 2022

Abstract

Background Bearing failure, the most frequent failure mode in rotating machinery is the typical mechanical fault. Such a failure might result in substantial financial losses at the workplace. One of the approaches made possible by other signal processing techniques is the early identification of various faults in rotating machinery; including bearing failures, misalignment, and others.

Purpose This fault is associated with many features used to diagnose different faults; thus, the Diagnostic Features (DF) is estimated at limited cyclic frequencies that refer to machine faults.

Method Two methods are used to extract the DF. The first one depends on time-domain features. The second is based on an advanced representation of the frequency domain, which depends on spectral coherence (SCoh) data over the spectral frequency domain using a center frequency and frequency range determined by a 1/3 binary tree structure. The calculated DFs are represented by a 2D map against the center frequency and frequency resolution. The maps from different fault features are collected to form the diagnostic patterns. The best characteristics connected to these various flaws can be found using statistical techniques like reverse arrangement tests (RAT). Artificial neural networks (ANN) may be trained and auto-diagnosed using the results from the best characteristics.

Results Using RAT is considered very important to summarize features. This method is given good results in training and diagnosis.

Conclusions Additionally, ANN and RAT provide a detection result of 100% based on the description of the machine's operating situation, whether it functioned commonly or incorrectly.

Keywords RAT · ANN · Time-domain feature · Rotating machine

Introduction

Features were employed in early failure detection techniques in the recent time domain. Depending on how well these elements can identify problems, some temporal domain (TD) characteristics are derived TAKÁCS [1]. By estimating the degradation trend in features over time with a cumulative approach, Kosasih et al. [2] were able to determine how the

slewing bearing was degrading. An autoregressive model was employed by James and Walter [3]. The retrieved characteristics are established to acquire a deterioration trend; the vibration signals could be changed when faults occur in rotating machinery Liu et al. [4]. The TD signals' amplitude and distribution may differ from the standard conditions. It is feasible to assess whether rotating machine damage is occurring using the TD statistical characteristics, according to Sreejith et al. [5]. The time and frequency domain can be used in feature extraction techniques by Chen et al. [6]. Bansal et al. [7] has presented a study comparing the performance of these three feature extraction methods (SIFT, SURF, and ORB), particularly when combined to recognize an object. The authors presented a comparative study of various feature descriptor algorithms and classification models for 2D object recognition. Bansal et al. [8] has extended their work to Combining in-depth features extracted using

✉ Mohammed Al-Saad
mohammed.kadom@uobasrah.edu.iq

Mohammed Al-Mosallam
mohammed.mohsen@uobasrah.edu.iq

Ahmad A. M. Alsahlani
Ahmad.mahdi@uobasrah.edu.iq

¹ Mechanical Department/Engineering College, Basrah University, Basrah, Iraq

VGG19 with handcrafted feature extraction methods, such as SIFT, SURF, ORB, and Shi-Tomasi corner detector algorithm, improving image classification performance.

Tsang [9] revealed the best way to discover the trend in data via a review. These data can be delivered separately and similarly. Additionally, the null hypothesis is promised these data. By integrating convolutional neural networks (CNNs) with variational mode decomposition (VMD) algorithms, processing raw vibration data directly without artificial intelligence or manual labor allowed Xu et al. [10] to complete the end-to-end defect detection of rolling bearings. Zhang et al. and Zhao et al. [11, 12]. They demonstrated how to leverage the CM and FDD to identify defects and failures in components. Beck et al. [13] review the statistical test procedures for determining the stationary of the surface electromyography (EMG) signal. A rat is used to symbolize one of these statistical techniques. Watson et al. [14] use rat to test the randomization hypothesis for each data set. Further, Murray et al. [15] also introduced rat for pattern recognition issues. They showed that the rat performs better than the support vector machine. In this work, we will put all of our efforts into using the rat approach to estimate the trend in features and identify the gradients in the data caused by a specific machine issue. Next, this cutting-edge technique finds and isolates spinning machine flaws.

The best machine fault detection techniques continue to be learning techniques like ANN. Using machine learning techniques, Attaran [16] looked into the issue of automated bearing defect diagnosis. These techniques focus on the TD statistical characteristic and encompass feature extraction, selection, and classification. Vibration signature analysis also uses different development methodologies. Sar et al. [17] introduced a review of current methods for developing vibration signatures.

This paper aims to use a numerical method to extract features issued with features in either a time or frequency domain depending on transforming signals to image representation, which is used to detect rotating machinery faults.

Time Domain Features

The following TD characteristics may be extracted from a raw vibration signal:

Mean Value

$$\text{Mean } \bar{x} = \frac{1}{N} \sum_{i=1}^N x(i) \quad (1)$$

In most cases, vibration analysis does not make much use of a signal's mean value. However, it showed how the vibration signal behaved.

Root Mean Square (RMS)

This function performs well in monitoring the signal's total vibration intensity Sar et al. [17]. Calculating the RMS value from the formula by Cuc et al. [18]:

$$\text{RMS} = \sqrt{\frac{1}{N} \sum_{i=1}^N x(i)^2} \quad (2)$$

Standard Deviation, SD

It is a measurement of the mean's dispersion. This is how the standard deviation is described:

$$\text{SD}, \sigma = \sqrt{\frac{1}{N} \sum_{i=1}^N (x(i) - \bar{x})^2} \quad (3)$$

Kurtosis

It indicates the extent of the distribution tail and identifies the most prominent peaks in the data set. Kurtosis is given by Cho et al. [19], Bhende et al. [20]:

$$\text{Kur} = \frac{\frac{1}{N} \sum_{i=1}^N (x(i) - \bar{x})^4}{\sigma^4} \quad (4)$$

Skewness

When studying dynamic signals, the term skewness (SK) is frequently utilized; SK is defined by Cho et al. [16],

$$\text{SK} = \frac{\frac{1}{N} \sum_{i=1}^N (x(i) - \bar{x})^3}{\sigma^3} \quad (5)$$

The value of x is increased to the third power because the SK reading is more sensitive to asymmetry in high x readings than the mean.

Peak Value

It is unquestionably a sign of component degeneration The PV is defined by Bhende et al. [20] and Benkedjough et al. [21] as:

$$\text{PV} = \frac{1}{2} (\max(x(i)) - \min(x(i))) \quad (6)$$

Shape Factor

The ratio of the RMS to the mean value is known as the shape factor (SF). It illustrates adjustments under misalignment and imbalance Benkedjough et al. [21].

$$SF = \frac{RMS}{\frac{1}{N} \sum_{i=1}^N |x(i)|} \tag{7}$$

Impulse Factor

The ratio of the peak value to the mean value of the time signal is known as the impulse factor (IMF), which is also a bearing defect indication Bhende et al. [20].

$$ImF = \frac{Peak}{\frac{1}{N} \sum_{i=1}^N |x(i)|} \tag{8}$$

Clearance Factor (CF)

Another time domain characteristic that Bhende et al. [20] can estimate is this one,

$$CF = \frac{Peak}{\frac{1}{N} \left(\sum_{i=1}^N \sqrt{|x(i)|} \right)^2} \tag{9}$$

Crest Factor

An impact estimate in a waveform can be calculated quickly using the CF formula. Wear-on gear teeth, cavitations, and roller bearings are frequently linked to impacting. One of the most important characteristics used to trend machine conditions is the CF Bendat and Peirsol [22]. CF is given below by Cho et al. [19]:

$$CrF = \frac{Peak}{RMS} \tag{10}$$

$x(i)$ is a signal series for $i = 1, 2 \dots N$, and N is the number of data points.

Signal Processing

Signal processing involves the processing, amplification, and interpretation of signals. Raw vibration signal always contains contamination components (“noise”) and frequently some basic components that may partially obscure other components that are the important part of the measurements taken. Several choices can have the noise or other uninterested signal parts removed. One is the time domain signal

averaging to attenuate the unsynchronized signal. The other option is to pass the raw signal through a filter and analyze the signal in the time or frequency domain. Another powerful indicator commonly used to measure the strength of correlation between the signal and its time-shifted version is the spectral coherence given in Eq. (11) Antoni [23]:

$$SCoh(f, \alpha) = \frac{S_{2X}(f, \alpha)}{\sqrt{S_{2X}(f, 0)S_{2X}(f - \alpha, 0)}} \tag{11}$$

where $S_{2X}(f, \alpha)$ is the spectral correlation function that represents the power distribution of the signal concerning its spectral frequency f , which can estimate from:

$$S_{2X}(f, \alpha) = \mathbb{E} \left\{ X(f + \beta\alpha)X(f - \bar{\beta}\alpha)^* \right\} \tag{12}$$

Moreover, cyclic frequency α and $X(f)$ represent the Fourier transform of the signal blocks. The SC function can be calculated using several techniques, such as the FFT accumulation method (FAM) Roberts et al. [24], averaged cyclic periodogram (ACP) Antoni [25], or fast spectral correlation (FSC), Antoni et al.[26], which can lead to producing the image representation form, as shown in Fig. 1?

Processing of Image using SIFT

The resulting image from spectral coherence analysis now deals with Scale Invariant Feature Transform (SIFT), a feature detection algorithm. SIFT also assists in finding the local features in an image, usually known as the 'key points of the image. These key points are scale & rotation invariants used for numerous pc vision applications. They can also be utilized in the fault designation method, which may be used in this text in machine fault diagnosis supported the image ensuing from reworking the time domain signal to image matching. We can also use the

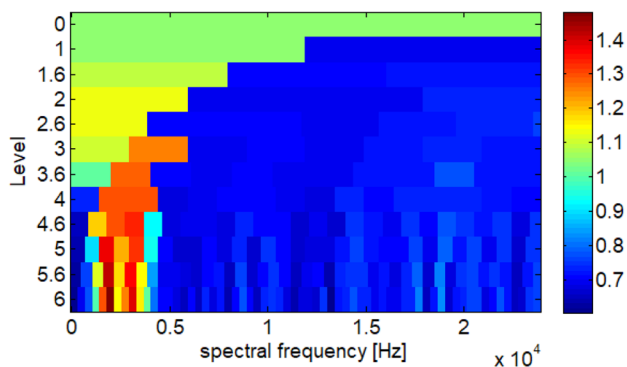
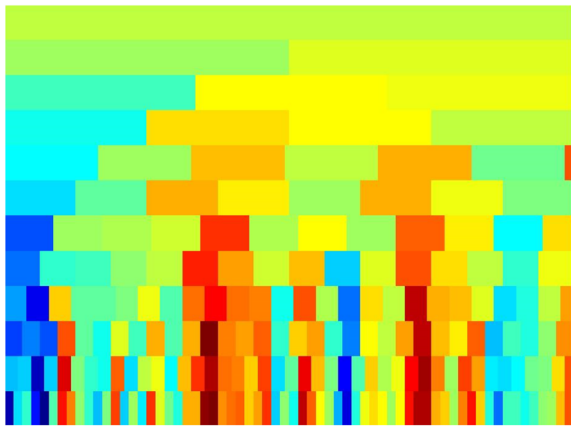


Fig. 1 Image representation form



Transferred to 256X256

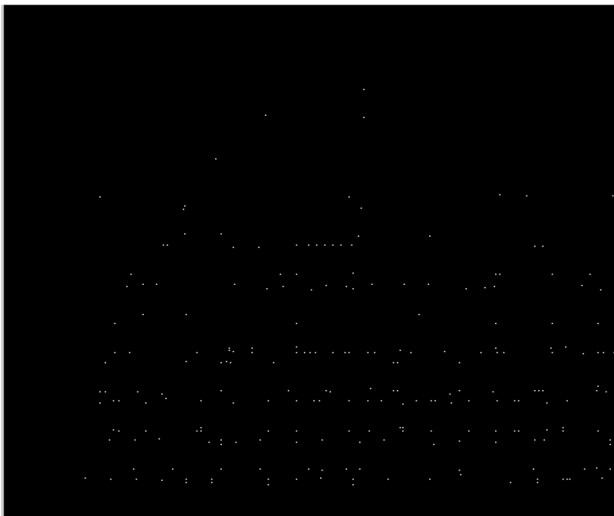
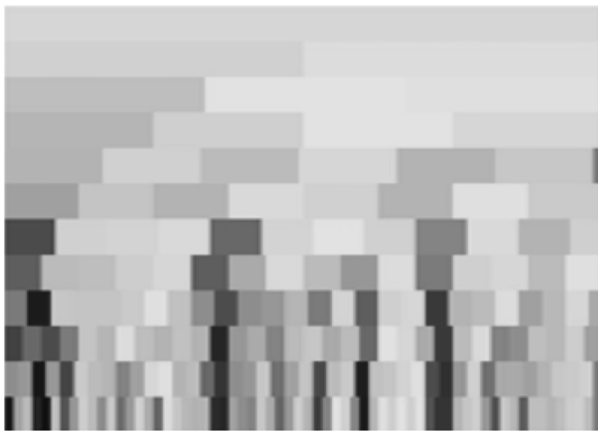


Fig. 2 Image representation of SIFT

key points generated using SIFT as features for the image during model training. The significant advantage of SIFT features, over edge features or hog features, is that they are not affected by the size or orientation of the image (Fig. 2).

RAT in Features Trend and Selection

The machine's healthy state is changed according to the features. As a result, changes in time-domain properties are frequently used to audit bearing deterioration. The incipient of the defect is found to be more accurate based on the extracted features than the retrieved characteristics from the original vibration signal Kosasih et al. [2]. Defect bearing displays a gradual upward trend and increases in variance over healthy bearing, and its magnitude is larger than healthy bearing Watson et al. [14]. In this part can be used a formalist statistical test. The test is excellent at detecting monotonic (i.e., gradual and continuing) trends in data. The existence of these trends also shows non-randomness. The existence of these trends also indicates non-randomness. The created test, a well-known accurate randomness test, was given by Bendat and Peirsol [22]. The rat considers a hypothesis test that looks for trends in the observed parameter Bendat and Peirsol [22]. Following is the test procedure:

First, consider the sampled time sequence of signal $x(t)$ of length $M \times N$, M measures, where N is the number of samples in each measurement. There are N segments in the series. The parameters are calculated using these segments. To examine their trend, several metrics are employed. The signal segment might be identified as. According to what was stated in part before. This technique tests the TD parameters that were previously described in the section that represented those parameters. The anticipated value owing to sample variations is then determined by computing a new function, h_{ij} , as Bendat and Peirsol [22] suggest. This is done to test the sequence of integers y_i associated with each parameter for changes outside:

$$h_{ij} = \begin{cases} 1 & \text{if } y_i > y_j \text{ for } j > i \\ 0 & \text{otherwise} \end{cases} \quad (13)$$

where $i = 1, 2, \dots, N - 1$, and $j = i + 1, i + 2, \dots, N$.

Calculating A_i factor for each number as:

$$A_i = \sum_{j=i+1}^N h_{ij} \quad (14)$$

The variable Several reverse arrangements can be estimated by:

$$A = \sum_{i=1}^{N-1} A_i \tag{15}$$

The two relevant equations Brandt [27] and Tsang [9] provide the mean and variance of an N-set of independent observations of a stationary random variable:

$$\mu_A = \frac{N(N - 1)}{4} \tag{16}$$

$$\text{var}_A = \frac{N(2N + 5)(N - 1)}{72} \tag{17}$$

$$Z = \frac{A - \mu_A}{\sqrt{\text{var}_A}} \tag{18}$$

Under this test's null hypothesis, the signal data points are shown as independent observations from random variables Beck et al. [13]. However, the alternate or renewal hypothesis demonstrated a relationship between the data points that make up the signal and an underlying pattern in a series of observations. If A falls inside Bendat and Peirsol's [22] range, the stationery hypothesis is accepted at the significance level of $\alpha = 0.05$:

$$A_{N;1-\alpha/2} < A \leq A_{N;\frac{\alpha}{2}} \tag{19}$$

The hypothesis is rejected at the α level of significance if the observed runs are outside the interval.

Artificial Neural Network

ANNs attempt to emulate their biological counterparts. ANNs have been developed in parallel distributed network models based on the human brain's biological learning

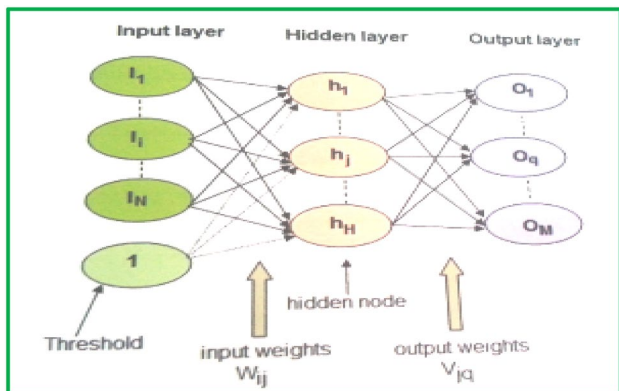


Fig. 3 Three-layer NN structure

process of the human brain Murray et al. [15]. Different methods can be used to deal with data in ANN applications. Multilayer receptor (MLP) neural networks are employed in this work since they are regarded as universal by the many forms of artificial neural networks Fig. 3 depicts the traditional three-layer feed-forward NN design.

For a network with N input nodes, H hidden nodes, and M output nodes, the mapping from the input vector (I1, ..., IN) to the output vector (O1, ..., OM) is given by:

$$O_q = g\left(\sum_{j=1}^H V_{jq}h_j\right) \tag{20}$$

where $q = 1, \dots, M$, V_{jq} is the weight from the hidden node (j) to the output node (q), and (g) is the activation function. The reading of hidden layer node h_j is given by:

$$h_{qj} = \sigma\left(\sum_{i=1}^N w_{ji} + b_j\right) \tag{21}$$

w_{ij} is the input weight, b_j is the threshold weight, and σ is the activation function which was chosen as the sigmoid function; that is very popular because it is monotonous, bounded, and has a simple derivative. Three steps comprise the general back propagation training: feed-forward of the input training pattern, back propagation of the related error, and weight modification.

In neural networks, sigmoid activation functions are commonly used. As it is monotonic and differentiable, each is needed for the back-propagation algorithm. Karlik and Olgac [28] give the equation for sigmoid functions:

$$J(s) = \frac{1}{1 + e^{-s_i}} \tag{22}$$

where s_i refers to the weighted sum.

Fault Detection Architecture

The suggested technique is depicted in a flow chart in Fig. 4. Its foundation is the integration of data from several sensors. Under two circumstances, the signals are taken from MFS. The first represents the machine's normal functioning situation, while the second is its broken state. A data capture system is used to transfer this data. The measured signal from four sensors is used to extract TD characteristics. Four places have these sensors installed (vertical and horizontal inboard and vertical and horizontal outboard). Then, rat examines the trend connected to each defect for the characteristics derived from the four sensors. The best feature is designated as one that affects any responsibility, while the rejected feature is designated as one with no impact on fault

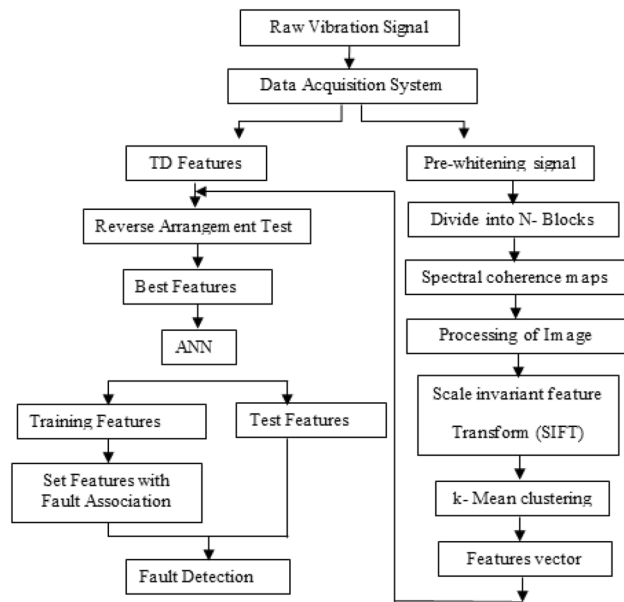


Fig. 4 Flow Chart of Proposed Method

change. To train the network, the best characteristics are sent into the system. Following the training process, each fault type's associated characteristics are categorized. Then, it is looked at how well the features pass the test and can detect errors. This technique is employed to find faults. The characteristics are diverse in their influence on each type of fault; hence all TD domain features should be analyzed to discover the optimum features connected with each fault.

Experimental Work

The suggested approach is validated using the Machinery Fault Simulator (MFS). method. 5. Study has been done on the bearing problems. These faults include ball and bearing wear and exterior and inner race faults. First-hand information about high-quality inboard and outboard rotor bearings may be gathered using the MFS. The device has to be

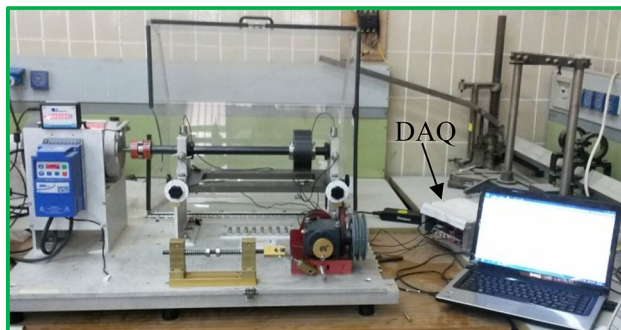


Fig. 5 MFS photography

correctly positioned. One at a time, a faulty bearing will be installed, and data will be gathered. The objective is to contrast the outcomes of suitable bearings with bad bearings. At 10 kHz, data is gathered. At 2700 RPM, the machine revolves (Fig. 5).

Results and Discussion

SIFT

The ensuing image from Spectral Coherence analysis for roller bearing of rotating machine as shown in Fig. 6 currently upset Scale Invariant Feature remodel (SIFT) as established in Fig. 6 to introduce SIFT operator to extract fault features from the recursive graphs. Following that, the most compelling feature of this fault is identified in rat for coaching or determining the fault; another case study involves outer race bearings, shown in Fig. 7 improves the image with entirely different features compared to either a traditional or faulty state.

As mentioned above, another case study on ball-bearing faults, as shown in Fig. 8, represents the Spectral Coherence of bearing faults. The work now yields the SIFT Fig. 9, representing the critical points generated using SIFT as features for the image during model training.

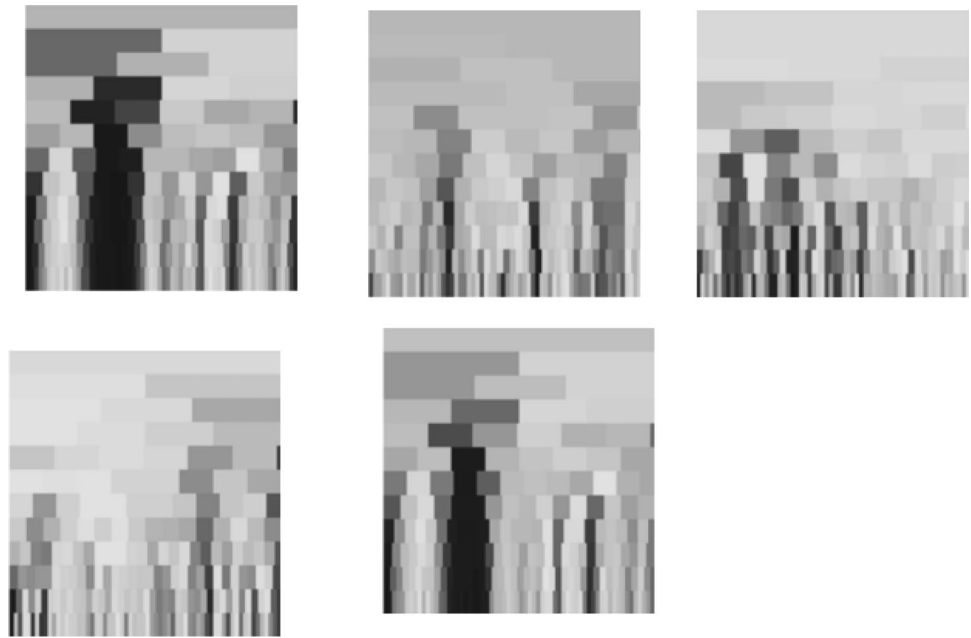
Then these produce the image that represents the key features associated with the traditional or faulty state.

The basic steps of the SIFT image registration algorithm are as follows: (1) Feature point extraction, (2) Generating feature descriptors, and (3) feature point matching. The feature point extraction mainly includes generating a difference of Gaussian (DOG) scale space, finding local extremum points, screening feature points, and determining the direction of feature points Wang et al. [29]

RAT

The best characteristics required to define the various bearing defects have been completed. The fault's most important features are selected to capture a data set at a rotating speed of 2700 RPM. Time-domain characteristics are determined for 10 reading sections for each rotation speed in the four directions (vertical Inboard VI, horizontal inboard HI, vertical outboard VO, and horizontal outboard HO). 4096 samples are taken per second at a sampling rate of 40,960 samples per reading. These data' rat is computed, as shown in Table 1. The rat indicator's acceptance values are AC, and its unacceptance values are UA. Time-domain Factors were shown to be less than ideal as a ball-bearing failure indicator, according to the results of rat. For this

Fig. 6 Spectral coherence outer fault



reason, it is essential to look for a new strategy to remedy this problem.

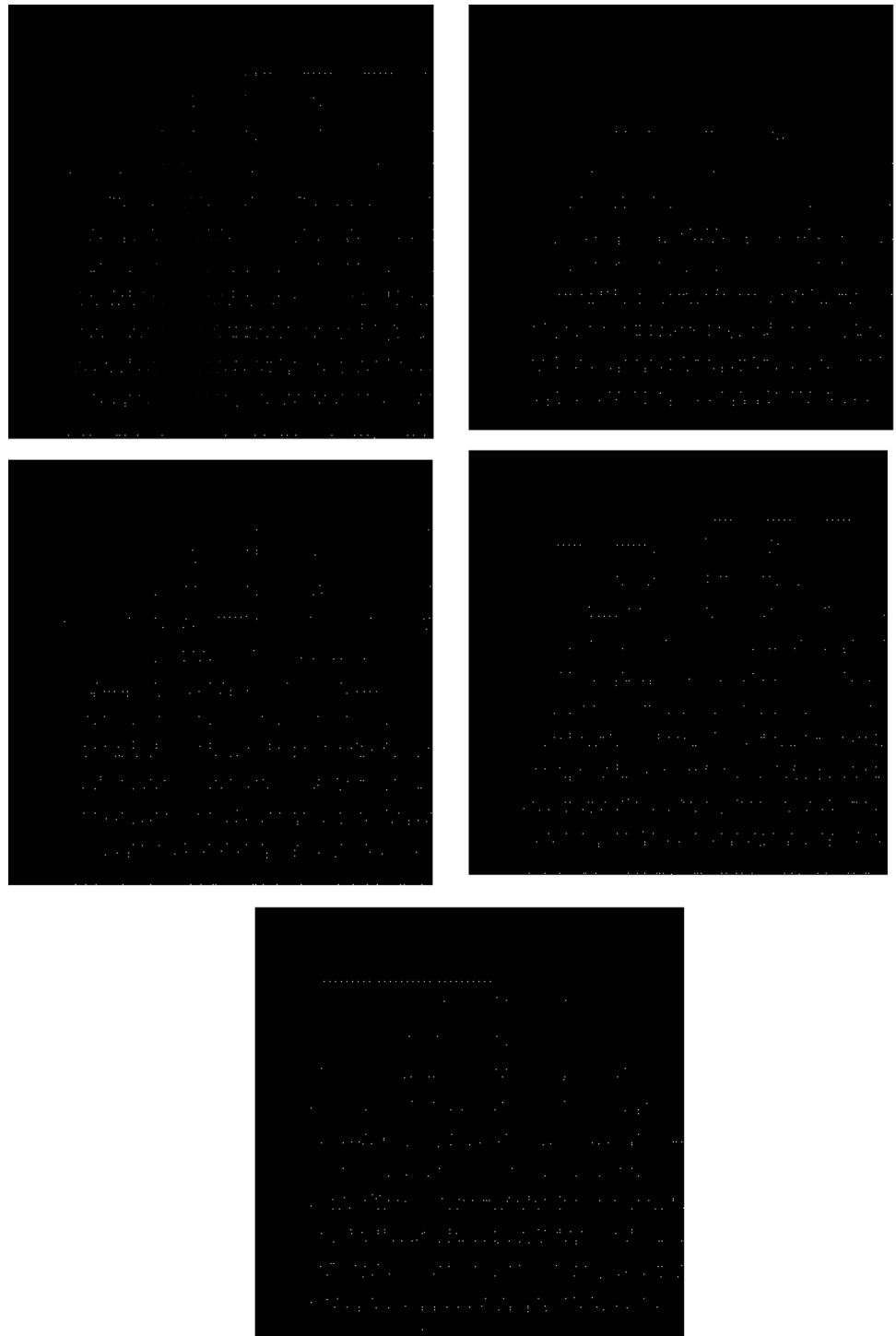
Nevertheless, would like to emphasize that Kurtosis, Shape, and Skewness still have an impact on fault identification since they provide indicators for condition prediction and fault diagnosis. Additionally, the horizontal and vertical directions, ranked by priority, are more effective in detecting ball faults. Kurt, form factor, and vertical order skewness were the more valuable criteria in identifying the inner race defect. These characteristics include kurtosis, skewness, impulsivity, and crest factors in the horizontal direction. As indicated in Table 2, these characteristics are assessed on the outboard or cage of the defective bearing, while the inboard cage continues to relate to the vibration signal. Here, we demonstrated how these characteristics might serve as an intelligent system's inputs. As a result of applying the rat method to identify the outer race fault, Table 3 confirmed the characteristics of Kurt, form factor, impulsiveness, and skewness on each vertical and horizontal axis, except for that within the horizontal path, the characteristics of the far crest component dominated so that the horizontal direction emerged as a result of the appropriate method for identifying the outer race fault. It is possible to deduce the rat compound fault table by looking at the three tables for each bearing fault.

Based on the vibration information of compound faults, as shown in Table 4, the rat of it determines the ruled path to be used to detect compound faults; Thus, the functions connected to this direction became RMS, well-known deviations, Kurt, shape, impulsive, clearance, and crest factors, as well as the form factor in the vertical course,

which should be examined in the intelligent machine to enhance fault detection capabilities. One may infer from the analysis of bearing faults that the fault impacts both inboard and outboard supports, which is evident from the tables. The study confined flaws, and the effect of a bearing problem did not cross over to other supports. This information will help with fault diagnostics.

ANN

The characteristics obtained from time domains are employed as input nodes in the input layer of the conventional three-layer NN. When the data corresponds to a normal operating condition (NOC), one node in the output layers has a value set to zero, while the output value refers to the defective operation situation (FOC). The primary software used to determine the NN weights is graphically written. The best NN design is [20-20-1], as shown in Table 5. The mean square error of the training technique is lowered by utilizing a varied number of nodes in the hidden layer (NHN), starting in training from 10 to 23 NHN. All of the characteristics that were retrieved from the time domain should be used since they have varied associations with various defect types. So that we may use those traits previously discovered and associated with various failures, the fault detection procedure cANNot make assumptions about a particular type of defect. To obtain disclosure problems for different types from a wide variety of data that could have specific deficiencies, the fault detection technique must be employed collectively. Identifying the rotating machine condition is beneficial even

Fig. 7 SIFT of the outer race

though the neural network training capacity may, at most, not reach 95%. As stated in Table 6, the NN approach for fault diagnosis is employed for validation with either NOC or FOC. Depending on the number of nodes in the hidden layer, their values may be evaluated using FOC using various examples. The machine being tested is shown in

the test case and in Fig. 10a, which is a training program component. The second Fig. 10b is for the scenario in which the machine breaks down. This program component, which will be used later to identify and forecast the kind of problem in rotary machines, is installed during the training process and tests a variety of data. It is part of the training process and not the finished program. This is

a step in verifying the program's ability to find errors and install the appropriate fixes, ensuring that it will function correctly during the fault detection process. The likelihood of identifying distinct defects utilizing this portion of the program has demonstrated encouraging results and

achieved 100% for specific errors. James and Walter assess the error's value [3]:

$$\% \text{ error} = \frac{[\text{act. value} - \text{est. value}]}{. \text{ value}} \times 100 \quad (23)$$

Fig. 8 Spectral coherence ball fault

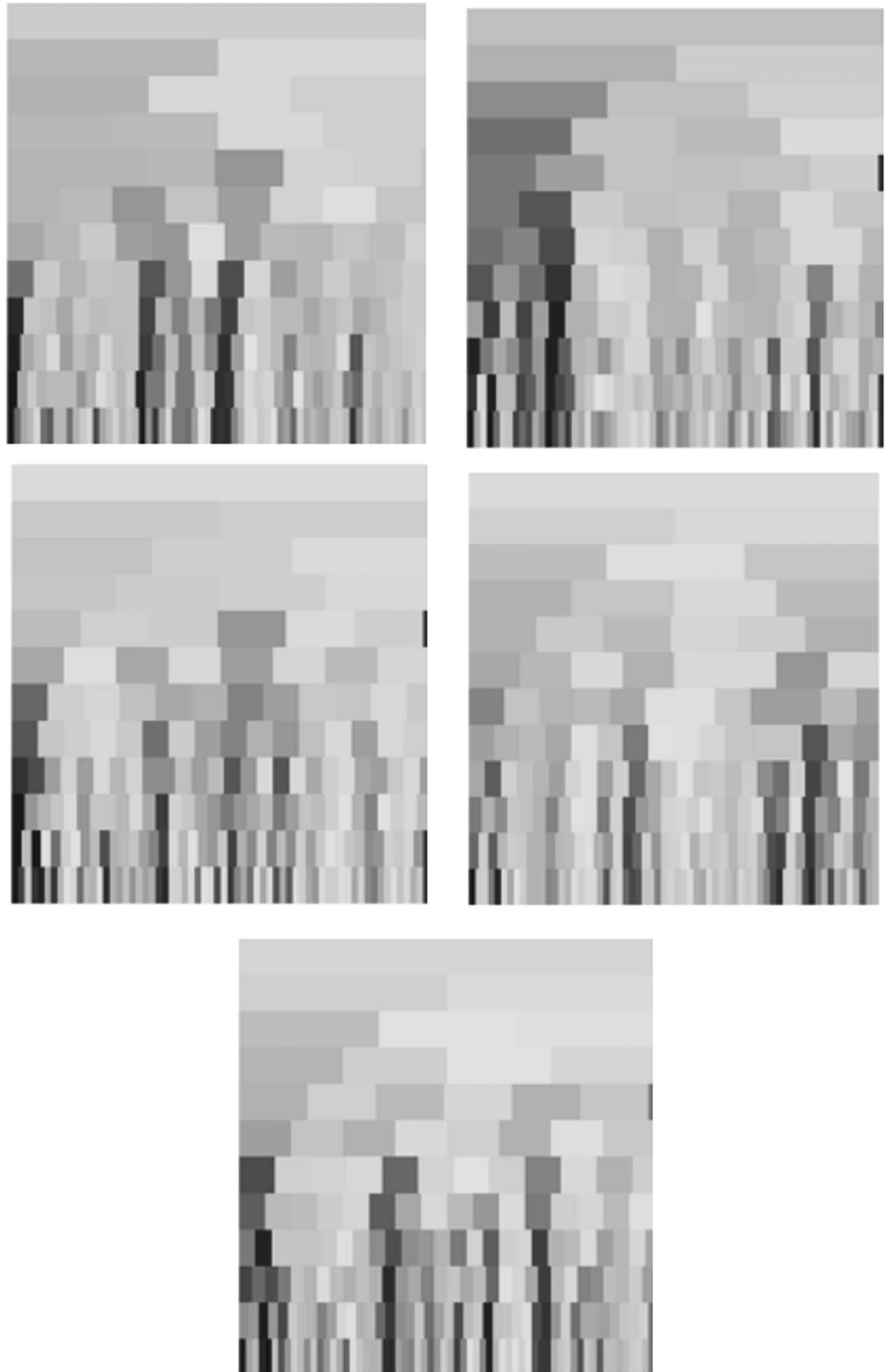
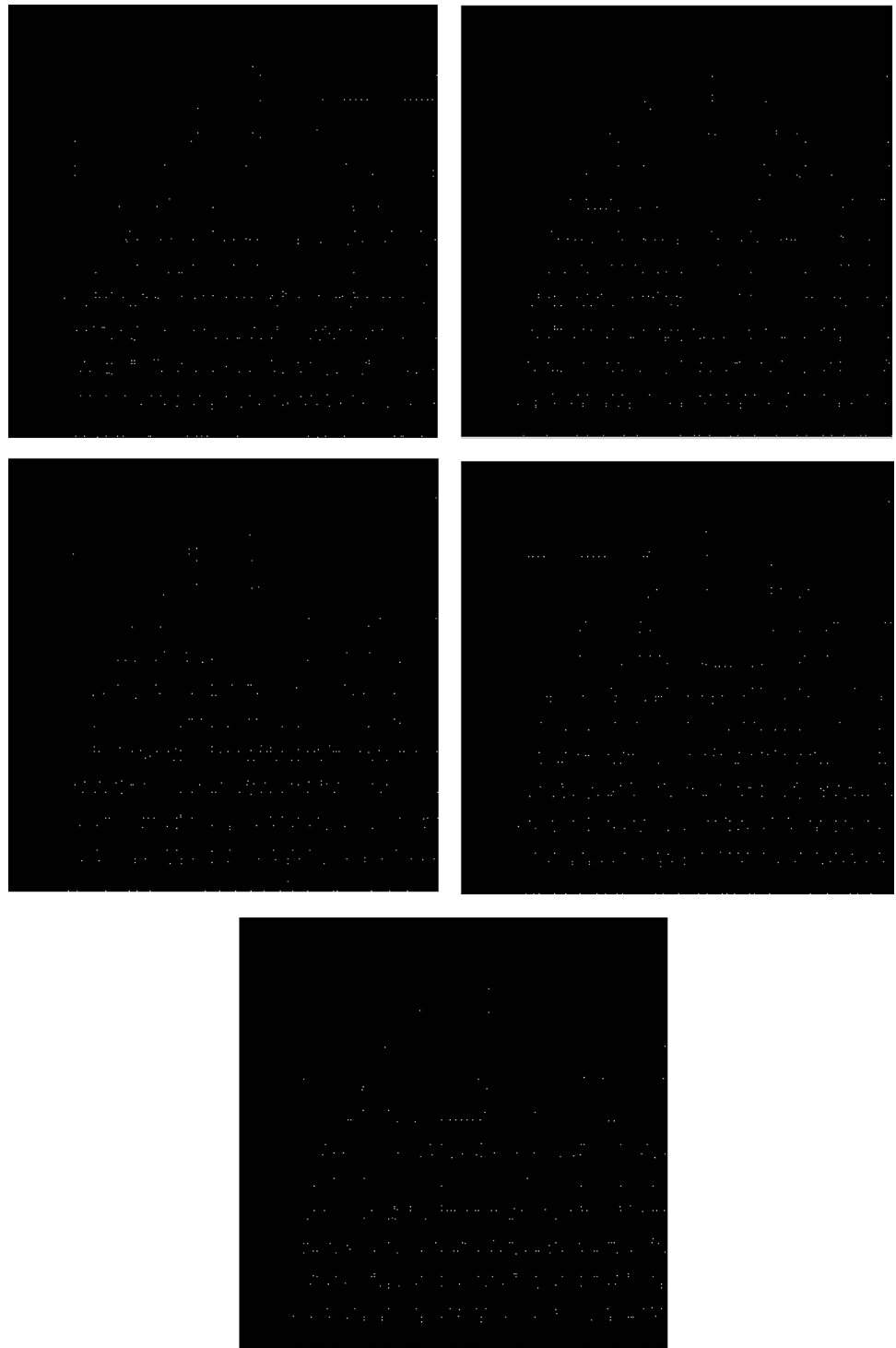


Fig. 9 SIFT ball fault

Training Error versus Epochs

When the number of cases increases and becomes more significant than four cases between NOC and FOC, the error estimated against the epoch numbers shows some fluctuation in their values. Still, in general, the degradation

trend towards approaching zero, It was demonstrated that things have a propensity to get smaller and smaller. These facts are explained in Figs. 11 and 12, also demonstrate how the minimum values are obtained as the number of epochs increases.



Table 1 Rat in TD factor for ball fault VI

	VO		HO		VI		HI	
Mean	7	UA	5	UA	8	UA	9	UA
RMS	8	UA	9	UA	9	UA	10	UA
SD	8	UA	9	UA	9	UA	10	UA
Kurt	20	AC	30	AC	42	UA	36	UA
Shap	20	AC	30	AC	44	UA	31	AC
Implsf	24	AC	31	AC	42	UA	41	UA
Clearcf	40	UA	41	UA	41	UA	40	UA
Crestf	25	AC	31	AC	42	UA	41	UA
Sk	10	UA	26	AC	34	AC	28	AC
Peak	11	UA	10	UA	10	UA	9	UA

Table 2 Rat for inner race fault in TD

	VO		HO		VI		HI	
Mean	3	UA	6	UA	11	UA	15	AC
RMS	7	UA	6	UA	7	UA	7	UA
SD	7	UA	6	UA	7	UA	7	UA
Kurt	31	AC	24	AC	44	UA	38	UA
Shap	22	AC	22	AC	41	UA	34	UA
Implsf	37	UA	21	AC	40	UA	39	UA
Clearcf	39	UA	38	UA	40	UA	37	UA
Crestf	36	UA	22	AC	40	UA	39	UA
Sk	33	AC	36	UA	26	AC	26	AC
Peak	9	UA	4	UA	6	UA	8	UA

Table 3 Rat for OUTER RACE FAULT in TD

	AC		HO		VI		HI	
Mean	UA	UA	3	UA	11	UA	22	AC
RMS	UA	UA	8	UA	5	UA	6	UA
SD	UA	UA	8	UA	5	UA	6	UA
Kurt	UA	AC	26	AC	42	UA	37	UA
Shap	UA	AC	19	AC	42	UA	33	UA
Implsf	UA	AC	31	AC	37	UA	38	UA
Clearcf	UA	UA	38	UA	39	UA	39	UA
Crestf	UA	UA	32	AC	37	UA	38	UA
Sk	UA	AC	23	AC	19	AC	43	UA
Peak	11	UA	9	UA	8	UA	7	UA

Comparison of Actual Value and ANN

The neural network operation prediction method outperformed the overall defect prognosis approach. The neural network is effectively used in differentiating defects because the difference between the real values and the neural network is relatively tiny. Figure 13 depicts the progression in data deterioration for bearings from the desired operating condition to a severe operation index for this bearing. These data cover the time period from 23/10 to 2/12, with a variety of bearings operating at 2700 RPM. The loading condition is

applied by screw tightening until a deep state is attained, in accordance with the ISO 10816-3 Vibration Severity Chart.

Conclusions

This work uses a novel method to detect the trend in features used in the bearing fault detection process. rat method has been influential in the extraction well and the necessary features associated with each failure independently and given sufficient accuracy in distinguishing

Table 4 Rat for Compound fault in TD

	VO		HO		VI		HI	
Mean	7	UA	2	UA	9	UA	3	UA
RMS	9	UA	19	AC	11	UA	10	UA
SD	9	UA	19	AC	11	UA	10	UA
Kurt	35	UA	19	AC	42	UA	41	UA
Shap	29	AC	13	AC	41	UA	33	AC
Implsf	39	UA	22	AC	41	UA	40	UA
Clearcf	40	UA	23	AC	39	UA	40	UA
Crestf	39	UA	23	AC	40	UA	40	UA
Sk	39	UA	38	UA	19	AC	22	AC
Peak	7	UA	8	UA	11	UA	8	UA

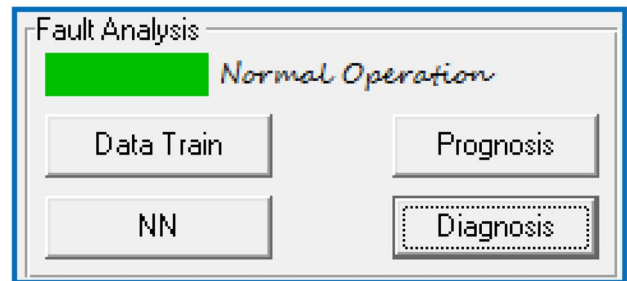
different types of defects. The TD features are chosen to identify the different types of faults in the rotating machine. The rat determines the relationship between fault and feature by examining the data trend for those alternatives. By analyzing the data associated with each failure, the rat technique has demonstrated that this data can be used to discover flaws. The machine's deterioration has been located. The rat discovered that not all fault kinds share the same criteria for identification. In other words, as indicated in all tables, each defect has specific characteristics. The best and most important approach for fault detection is considered to be ANN. The statement of machine operation status is detected by ANN with a detection rate of 100%, whether it is operating normally or not.

Table 5 Training of NN

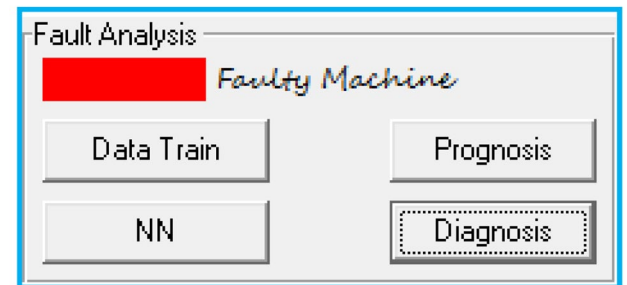
NHN	Estimated value	Actual value	Time consumption (sec)	Total no. of training
10	0.8164	1	12.73	800
15	0.7894	1	15.04	800
17	0.8039	1	15.04	800
20	0.9527	1	19.67	800
21	0.9425	1	20.83	800
23	0.9266	1	20.83	800

Table 6 Diagnosis of different cases Using NN

NHN	Estimated value	Actual value	Percentage Error %
10	0.1882	0	18.82
15	0.0952	0	9.52
17	0.0661	0	6.61
20	0.0565	0	5.65
21	0.0511	0	5.11
23	0.1015	0	10.15



(a) Normal Operation Case



(b) Faulty Machine State

Fig. 10 Machine Operation condition

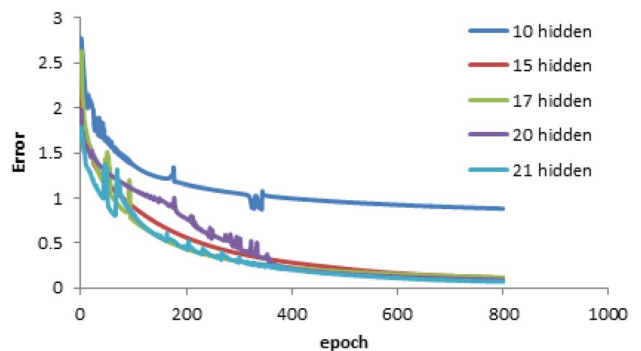


Fig. 11 Error against the epochs for 100 iterations and 4 cases

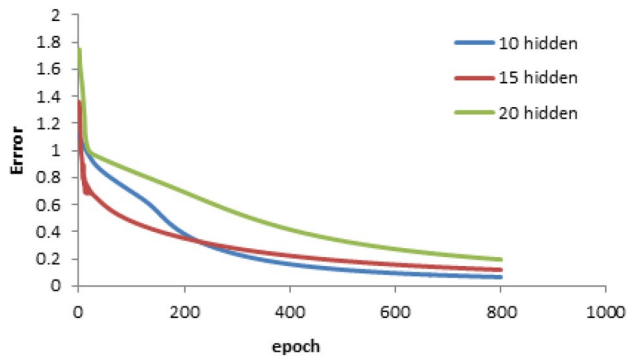


Fig. 12 Error against the epochs for 800 iterations and 8 cases

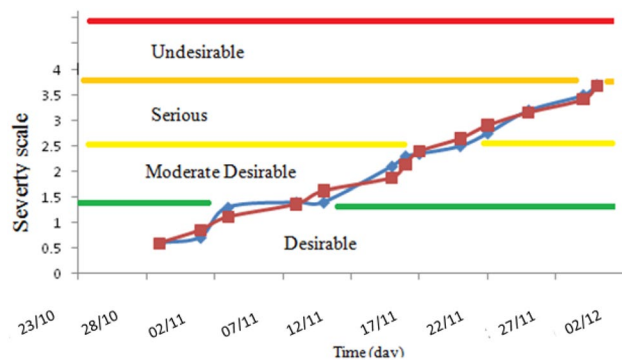


Fig. 13 Comparison actual value and ANN

References

- Takács DTASG (2022) Vibration analysis techniques for rolling element bearing fault detection. *Design Mach Struct*:65
- Kosasih BY, Caesarendra W, Tieu K, Widodo A, Moodie CA, Tieu AK (2014) Degradation trend estimation and prognosis of large low speed slewing bearing lifetime. *Appl Mech Mater*. <https://doi.org/10.4028/www.scientific.net/AMM.493.343>
- Kimotho JK, Sextro W (2014) An approach for feature extraction and selection from non-trending data for machinery prognosis. In: PHM Society European Conference
- Liu Z, Cao H, Chen X, He Z, Shen Z (2013) Multi-fault classification based on wavelet SVM with PSO algorithm to analyze vib. *Neurocomputing* 99:399–410
- Sreejith B, Verma A, Srividya A (2008) Fault diagnosis of rolling element bearing using time-domain features and neural networks. In: 2008 IEEE region 10 and the third international conference on industrial and information systems. IEEE.
- Chen J, Xu B, Zhang X (2021) A Vibration Feature Extraction Method Based on Time-Domain Dimensional Parameters and Mahalanobis Distance. *Math Probl Eng*: 2021
- Bansal M, Kumar M, Kumar M (2021) 2D object recognition: a compa. *Multimed Tools Appl* 80(12):18839–18857
- Bansal M, Kumar M, Sachdeva M, Mittal A (2021) Transfer learning for image classification using VGG19: Caltech-101 image data set. *J Ambient Intell Hum Comput*: 1–12.
- Tsang AH (2012) A review on-trend tests for failure data analysis. *West Indian J Eng* 35(1):4–9
- Xu Z, Li C, Yang Y (2020) Fault diagnosis of the rolling bearing of wind turbines based on the variational mode decomposition and deep convolutional neural networks. *Appl Soft Comput* 95:106515
- Zhang Y, Li X, Gao L, Chen W, Li P (2020) Intelligent fault diagnosis of rotating machinery using a new ensemble deep auto-encoder method. *Measurement* 151:107232
- Zhao X, Jia M, Lin M (2020) Deep Laplacian auto-encoder and its application into imbalanced fault diagnosis of rotating machinery. *Measurement* 152:107320
- Beck TW, Housh TJ, Weir JP, Cramer JT, Vardaxis V, Johnson GO, Coburn JW, Malek MH, Mielke M (2006) An examination of the runs test, reverse arrangements test, and modified reverse arrangements test for assessing surface EMG signal stationarity. *J Neurosci Methods* 156(1–2):242–248
- Watson M, Sheldon J, Amin S, Lee H, Byington C, Begin M (2007) A comprehensive high-frequency vibration monitoring system for incipient fault detection and isolation of gears, bearings, and shafts/couplings in turbine engines and accessories. In: *Turbo Expo: Power for Land, Sea, and Air*.
- Murray JF, Hughes GF, Kreutz-Delgado K (2003) Hard drive failure prediction using non-parametric statistical methods. In: *Proceedings of ICANN/ICONIP*
- Attaran B, Ghanbarzadeh A (2014) Bearing fault detection based on maximum likelihood estimation and optimized. *J Appl Comput Mech* 1(1):35–43
- Sar SK, Kumar R (2015) Techniques of vib. *Int J Adv Res Comput Commun Eng* 4(3):240–243
- Cuc AI (2002) Vib. University of South Carolina Columbia, SC
- Cho S, Binsaeid S, Asfour S (2010) Design of multi-sensor fusion-based tool condition monitoring system in end milling. *Int J Adv Manuf Technol* 46(5):681–694
- Bhende AR, Awari DG, Untawale DS (2012) Critical Review of Bearing Fault Detection Using Vibration Signal Analysis. *Int J Tech Res Dev* 1(1).
- Benkedjough T, Medjaher K, Zerhouni N, Rechak S (2012) Fault prognostic of bearings by using support vector data description. In: 2012 IEEE Conference on Prognostics and Health Management. IEEE.
- Bendat JS, Piersol AG (2011) *Random data: analysis and measurement procedures*, vol 729. Wiley
- Antoni J (2007) Cyclic spectral analysis in practice. *Mech Syst Signal Process* 21(2):597–630
- Roberts RS, Brown WA, Loomis HH (1994) Computationally efficient algorithms for cyclic spectral analysis. *IEEE Signal Process Mag* 8(2):38–49
- Antoni J (2009) Cyclostationarity by examples. *Mech Syst Signal Process* 23(4):987–1036
- Antoni J, Xin G, Hamzaoui N (2017) Fast computation of the spectral correlation. *Mech Syst Signal Process* 92:248–277
- Brandt A (2011) *Noise and vibration analysis: signal analysis and experimental procedures*. John Wiley & Sons.
- Karlik B, Olgac AV (2011) Performance analysis of various activation functions in generalized MLP architectures of neural networks. *Int J Artif Intell Expert Syst* 1(4):111–122
- Wang Y, Zhou B, Cheng M, Fu H, Yu D, Wu W (2019) A fault diagnosis scheme for rotating machinery using recurrence plot and scale-invariant feature transform. In: *Proceedings of the 3rd International Conference on Mechatronics Engineering and Information Technology (ICMEIT 2019)*

Publisher's Note Springer Nature remains neutral with regard to jurisdictional claims in published maps and institutional affiliations.

Springer Nature or its licensor holds exclusive rights to this article under a publishing agreement with the author(s) or other rightsholder(s); author self-archiving of the accepted manuscript version of this article is solely governed by the terms of such publishing agreement and applicable law.